ChemComm

COMMUNICATION

View Article Online
View Journal | View Issue

Cite this: *Chem. Commun.*, 2025, **61**, 14665

Received 9th June 2025,
Accepted 7th August 2025

DOI: 10.1039/d5cc03245h

rsc.li/chemcomm

Visible light promoted oxygenation of oxazolidinones by an anthraquinone-resorcinol based donor–acceptor polymer as a heterogeneous photocatalyst

Bubun Nayak,† Shiladitya Roy,† Devendra Mayurdhwaj Sanke, Ajay Vinayakrao Munde and Sanjio S. Zade *

The direct conversion of 2-oxazolidinone to oxazolidine-2,4-dione can be achieved by C(sp^3)–H bond activation using a heterogeneous photocatalyst. Here, a donor–acceptor (D–A) conjugated heterogeneous polymer (ACP) was employed as an efficient photocatalyst for the oxidation. Upon light irradiation, ACP functions as a photo-base and facilitates the reaction *via* a proton-coupled electron transfer (PCET) mechanism.

The oxazolidine-2,4-dione is a prevalent structural feature in natural products, with a wide range of biological activities, such as anticonvulsant,[1] anti-inflammatory,[2] antibacterial,[3] fungicide,[4] and mineralocorticoid receptor (MR) antagonist activity (Fig. 1).[5]

Gramain *et al.* were the first to report the UV-light-induced photooxidation of 2-oxazolidinone.[6] Later, the electrochemical approach was used to oxidize 2-oxazolidinone *via* fluorination. However, the above two direct processes have limited applications due to the use of UV light and high current density in fluidic solutions with low yields.[7] Then, Galushchinskiy *et al.* reported another approach to oxidize the methylene group using mpg-CN as a photocatalyst.[8] However, this process has the drawback of low oxidation yield of substrates and harsh conditions for catalyst synthesis.

Photocatalytic C–H bond cleavage *via* hydrogen atom transfer (HAT) has been observed with organic dyes such as Eosin Y,[9] 9-fluorenone,[10] 2-chloroanthraquinone,[11] and xanthone.[12] In these systems, the photocatalyst is excited upon light irradiation and subsequently abstracts a hydrogen atom from the substrate.[13,14] Anthraquinone (AQ) and its derivatives exhibit remarkable versatility in mediating a variety of transformations,[15] including C–H functionalization,[16] C–X bond cleavage,[17] and C–H bond oxidation.[18] In general, the efficiency of these reactions depends on several factors such as substrate functionality (bond dissociation energy, radical stability), abstractor nature, and solvent.[19] AQ is photoexcited upon absorption of 350–450 nm light and undergoes intersystem crossing (ISC), with the second triplet excited state (T_2) lying close in energy to the first singlet excited state (S_1) (ϕ_T = 0.72, ΔE = 1.5 kcal mol^{-1}).[20] The anthraquinone-based photocatalysts in their excited state can also mediate ET (energy transfer),[21] PET (photoinduced electron transfer),[22] and PCET (proton-coupled electron transfer).[23] However, in the absence of an external organic base, most AQ-based catalysts operate *via* HAT. The key features of AQ-based photocatalysts include: (i) tunability of absorption and redox properties through substitution on the AQ core, (ii) participation in both oxidative and reductive catalytic pathways, and (iii) high photostability, making them suitable for long-term catalysis.

Herein, we employed an anthraquinone-resorcinol coupled heterogeneous polymer (ACP), where AQ serves as a redox-active center, and resorcinol reduces the band gap through a charge transfer pathway. The photocatalyst absorbs the visible part of the light (λ_{max} = 456 nm) and efficiently converts 2-oxazolidinone to oxazolidine-2,4-dione with good yield. The photocatalytic transformation proceeds through a PCET, in which the catalyst acts as a photo-base and selectively breaks the C(sp^3)–H bond in oxazolidine-2-ones to form a desired product after reaction with oxygen.

The photocatalyst ACP was synthesized by a solvothermal process using 2,6-bis(chloromethyl)anthraquinone (**6**) and resorcinol in ethanol–water (EtOH–H_2O) in the presence of ammonia and characterized (Scheme 1 and Fig. S1, SI).[24] The solid-state photoluminescence study of the ACP catalyst shows the emission maxima at 581 nm (Fig. S2(a), SI), and the energy corresponding to the singlet state is 2.13 eV. A time-correlated single photon

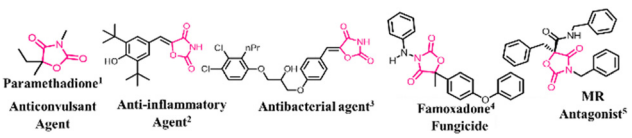

Fig. 1 Examples of biological activity of oxazolidinedione-containing molecules.[1–5]

Department of Chemical Sciences and Centre for Advanced Functional Materials, Indian Institute of Science Education and Research (IISER) Kolkata, Mohanpur, Nadia 741246, West Bengal, India. E-mail: sanjiozade@iiserkol.ac.in
† Equal contributing authors.

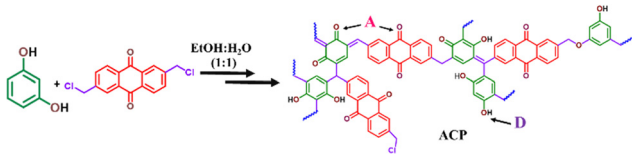

Scheme 1 Schematic representation of the synthesis of the anthraquinone–resorcinol conjugated polymer (ACP) by polycondensation reactions.

counting (TCSPC) study (Fig. S2(b), SI) for photoluminescence reveals an average lifetime of 6.78 ns (Table S1, SI). Secondary amides are typically more readily oxidized than tertiary amides because they facilitate proton abstraction or migration to oxygen.[25,26] Certain synthetic strategies take advantage of forming *N*-acylimines during the oxidation process.[27,28] Consequently, although oxygenating tertiary amides is synthetically challenging, research efforts have been directed toward developing methods suitable for both *N*-substituted and unsubstituted substrates. Initial optimization involved testing a series of heterogeneous and homogeneous catalysts. The reaction was carried out in acetonitrile solvent under an oxygen atmosphere and visible light irradiation (Table S2, SI). The highest yield of oxazolidinedione **2c** (55%, isolated) was obtained with the ACP heterogeneous photocatalyst. In contrast, molecular sensitizers such as Rose Bengal, Rhodamine B, and Eosin Y produced significantly lower yields of **2c**. This can be attributed to carbonyl and/or carboxyl functionalities in their structure, which may enable PCET from **1c** in the absence of the external base. Notably, the excited state of Eosin Y was identified as a direct hydrogen atom transfer (HAT) agent.[9] Although benzophenone has previously been reported to oxidize **1a**, possibly through interaction between the amide NH and its carbonyl group, it failed to produce **2c** with a good yield. As a photocatalyst, AQ was also ineffective in producing **2c** with a good yield. Additional screening was performed using AQ derivatives such as 1,8-dichloroanthraquinone, 1,8-dihydroxyanthraquinone, and 1,4-diaminoanthraquinone. However, none of these were successful in producing **2c** with a reasonable yield. A control experiment performed under a nitrogen atmosphere confirmed the crucial role of oxygen in the reaction. The reaction did not proceed without ACP and 456 nm irradiation. However, irradiation at 390 nm with a UV LED in the absence of ACP gave **2c** with a 17% yield (photochemical process). In the presence of the catalyst and illumination with a Tuna Blue LED, the yield of **2c** increased to 60% after 24 h. The green LED gives less conversion because of less absorption of green light (λ = 520–560 nm) by ACP. However, a white LED is able to produce **2c** with a 50% yield. Among the solvents tested, acetonitrile is the most suitable solvent to perform oxygenation of oxazolidinone **1c** under Tuna Blue LED illumination, likely due to polarity, quenching power, chemical stability, and inert nature in the reaction conditions.

With the optimized reaction conditions using ACP as the catalyst and acetonitrile as a solvent, the reaction was performed with 0.5 mmol of the substrate with a series of oxazolidinones **1a–t** (Fig. 2). The primary objectives were (i) to establish a general protocol applicable for a broad range of substrates, including those with and without *N*-aromatic groups, and (ii) to investigate the role of ACP as a heterogeneous photocatalyst. The substrate scope

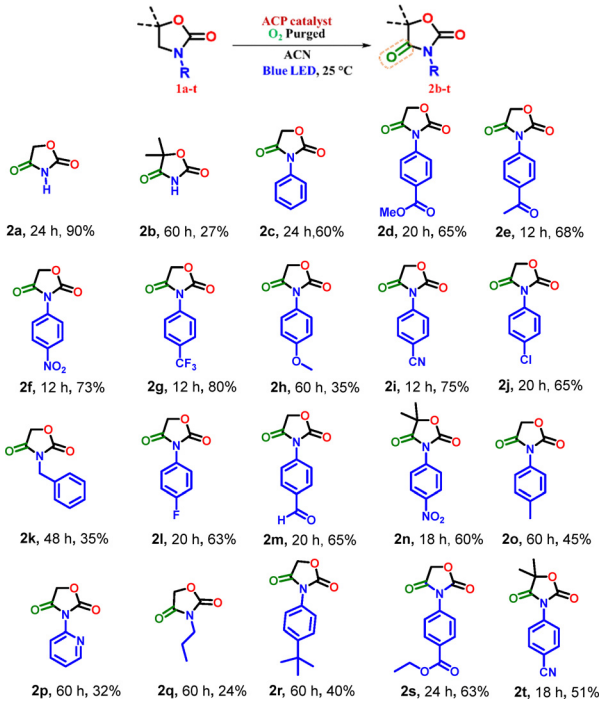

Fig. 2 Scope of oxazolidinones used for scaled-up oxidation. Reaction conditions: 1 (0.5 mmol), O_2, acetonitrile (6 mL), ACP (55 mg), Tuna Blue LED (34 W), 25 °C. Percent values indicate isolated yields. Synthetic procedures of the precursor molecules and oxidation products, as well as ^{1}H and ^{13}C NMR spectra, are given in the SI.

demonstrated excellent yield for unsubstituted oxazolidinone **1a** and moderate to good yields for *N*-substituted derivatives of oxazolidinones and 5,5-dimethylated oxazolidinones. The substrate scope clearly showed that *N*-phenyl-substituted substrates with electron-withdrawing groups at the para position produced higher yields and required shorter reaction times than those with electron-donating groups. Electron-rich groups, such as the 4-methoxyphenyl fragment in **1h**, showed typical behaviour of the 4-methoxyphenyl (PMP) protecting group when attached to the amine or amide functionality; it was readily cleaved under the photocatalytic conditions. Oxygenation of **1h** gives the desired product **2h** (35%) along with PMP-deprotected oxazolidinedione **2a**. The yield was significantly lower in the 5,5-dimethylated substrates like **1b**, **1n**, and **1t** than in those without substituents at the 5-position. For *N*-alkylated oxazolidinone **1q**, the yield was also low. The product selectivity was also lower due to competitive oxygenation of *endo*- and *exo*-CH_2-groups in **1q** and formation of **2q′** (yield: 20%, see SI, Section S2.5) as a side product. Previous reports indicated that the Br$^\bullet$ radical abstracts hydrogen in cyclic amides at both the *endo*- and *exo*-CH_2 positions, with a higher preference for the former.[29] *N*-Benzyl substituted oxazolidinone gave the desired product **2k** (yield: 35%) with a low yield and major formation of **2k′** (yield: 42%, see SI, Section S2.5) as a side product by the oxidation of the *exo*-CH_2-group. The relatively low yield for *N*-benzyl substituted oxazolidinone is due to the potential overoxidation of **1k**.[30] For substrate **1o**, there is oxidation on the methyl group also to form **1m** (yield: 20%) and its oxidised product **2m** (yield: 5%).[31]

There are three possible processes to take into account: (1) the substrate reacts with singlet oxygen, (2) the substrate undergoes direct oxidation through PET, or (3) a carbon-centered radical is generated *via* PCET. One of the possibilities of oxygen activation is the formation of singlet oxygen by the energy transfer (ET) pathway. However, screening of other well-known efficient singlet oxygen-generating catalysts, such as Rose Bengal, methylene blue, Eosin Y, and rhodamine B, gave a lower yield of target oxazolidinedione than ACP. This serves as evidence that the ET pathway is unlikely to be the major pathway. The heterogeneous catalyst ACP accomplished a higher yield, likely due to the involvement of PCET. The reduced yield observed for 5-substituted oxazolidinones (**1b**, **1n**, and **1t**) suggests a direct interaction between the substrate and the catalyst, with steric hindrance playing a significant role in reducing the efficiency of the reaction. Such spatial interference is unlikely to be an issue if a small molecule, such as $^1O_2$, were the one interacting with the substrate. Cyclic voltammetry experiments were performed to rule out the involvement of the PET process in the reaction mechanism of ACP (Fig. S3, SI). The oxidation potentials of **1c**, **1h**, and **1i** are reported as 1.58 V, 1.26 V, and 1.91 V_{SCE} (at half peak), respectively.[8] In comparison, the oxidation potential of ACP is 1.1 V_{SCE} (at half peak, Fig. S3, SI), which unambiguously indicates that PET from oxazolidinones to ACP is thermodynamically unfavourable.

The conduction band potential of ACP was calculated to be 0.31 V_{RHE}, which is inadequate to transfer an electron to ground-state oxygen ($^3O_2$) to form a superoxide radical anion ($O_2^{\bullet -}$, -0.33 V_{RHE}).[24] Hence, the catalyst cannot generate a superoxide radical anion *via* the PET pathway to drive substrate oxidation. The generation of reactive oxygen species in the reaction medium was confirmed by the formation of anthraquinone from anthracene (Fig. S50, SI), benzaldehyde from benzyl alcohol (Fig. S52, SI), and a decrease in overall yield of oxazolidine-2,4-dione (55%) by adding *p*-benzoquinone (SI: 3.3). To confirm the generation of singlet oxygen, we performed the transformation under 390 nm light without ACP (SI: 3.4). The light at this wavelength can provide the energy to change the spin state of O_2. However, a significantly lower product yield was observed under these conditions, which indicates that singlet oxygen generation is inefficient in the absence of the catalyst. Thus, the catalyst is crucial for the generation of singlet oxygen. A gradual decrease in photoluminescence (PL) intensity (Fig. S5, SI) was observed upon batch-wise addition of 200 μM 2-oxazolidinone to the catalyst solution, and the quenching rate constant was found to be 2.62×10^2 M^{-1} from the Stern–Volmer plot (Fig. S5, SI). Thus, all these results indicate that the oxidation may occur *via* a PCET pathway.

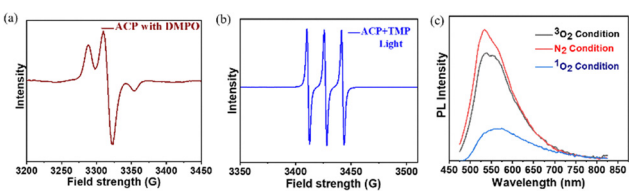

Fig. 3 (a) ESR spectra of ACP with DMPO after light irradiation, (b) ESR spectra of ACP with TMP after light irradiation for *in situ* TEMPO generation, and (c) PL spectrum of ACP at three different conditions in the solution state.

Electron spin resonance (ESR) spectroscopy was used to check the generation of reactive oxygen species (Fig. 3). Fig. 3(a) suggests that the ACP is unable to generate superoxide radical anions ($O_2^{\bullet -}$). However, the ACP catalyst generates a TEMPO radical from TMP after blue light irradiation for 30 minutes, as evidenced by ESR spectroscopy (Fig. 3(b)). This study confirms the generation of singlet oxygen ($^1O_2$) by the ACP catalyst. A solution-state fluorescence quenching study also supports the generation of singlet oxygen by the ACP catalyst (Fig. 3(c)).

The ESR spectrum of ACP, with a "*g*" value of 2.002, confirms the presence of unpaired π-electrons within its polymer framework.[24] When the ACP photocatalyst is exposed to visible light, the intensity of the ESR signal increases, providing evidence that photoexcitation encourages the splitting of excitons, leading to the formation of charge carriers (h^+ and e^-). The electron–hole pair separation becomes faster and easier due to the presence of the alternate D and A units in the polymeric chains. The e^- mostly settles in the quinone unit, while the hole h^+ finds its place on the resorcinol unit. The electron on the quinone moiety abstracts a proton from the substrate, while the hole on the resorcinol unit accepts an electron simultaneously. The catalyst exhibits properties like phenoxide ions due to localized e^- on the quinone unit; the formed radical on the carbon of the carbonyl group becomes stable by forming a benzylic radical through conjugation, which becomes highly stable due to conjugation with the anthraquinone unit. As a result, the excited state of the catalyst (ACP-m*) behaves as a photo base and abstracts one H^+ from the endocyclic C–H bond in a β-position to the amide nitrogen of **1a′**, leading to the formation of C-centered radical **1a′A**, and simultaneously takes one electron from the substrate, and forms a stable hydrogenated radical [ACP-m + H]$^\bullet$. Radical **1a′A** was detected by HRMS analysis of the crude reaction mixture using both TEMPO and BHT as a trapping agent (Fig. S6, S7; details in SI S5). The formed radical **1a′A** then reacted readily with the molecular oxygen present in the reaction medium, instead of undergoing one electron transfer from C-centered radical **1a′A** to form the corresponding iminium ion intermediate. The formation of an iminium ion intermediate from **1a′A** requires high energy, as the formation of an ionic intermediate from a neutral species is an endothermic process. On the other hand, the removal of one electron from the *N*-atom of cyclic amide moieties is also highly challenging. Oxazolidinones have peak potential $E_p > 1.67$–2.72 V_{SCE}, which confirms their stability against oxidation.[8] Therefore, due to all these responsible factors, **1a′A** undergoes trapping by molecular oxygen readily to generate neutral peroxo radical **1a′B**. The peroxo radical **1a′B** recovers the H-atom from the hydrogenated radical [ACP-m + H]$^\bullet$ and creates a hydroperoxide intermediate **1a′C** from which a water molecule gets eliminated, and the desired product **2b′** is produced (Fig. 4). Finally, FE-SEM morphological analysis (Fig. S55(c), SI) and FT-IR analysis (Fig. S55(a) and (b), SI) of the photoirradiation (24 h) demonstrated that the aggregated nanoparticles retained their globular shape.

The catalyst selectively cleaves the endocyclic C–H bond at the β-position relative to the amide nitrogen in compound **1a′** because this proton is relatively more acidic. Thus, when the *N*-atom of oxazolidinone is bonded to an electron-withdrawing aromatic moiety, the acidity of that proton further increases; as

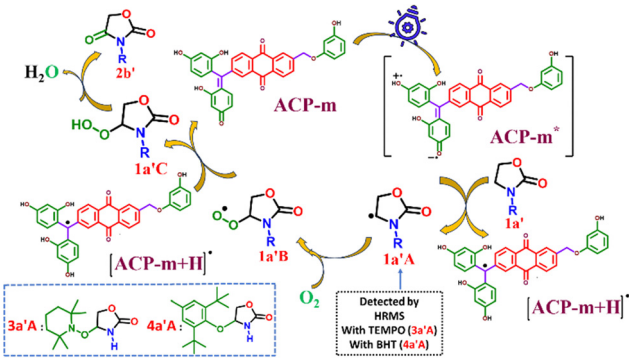

Fig. 4 Plausible mechanism of 2-oxazolidinone oxidation.

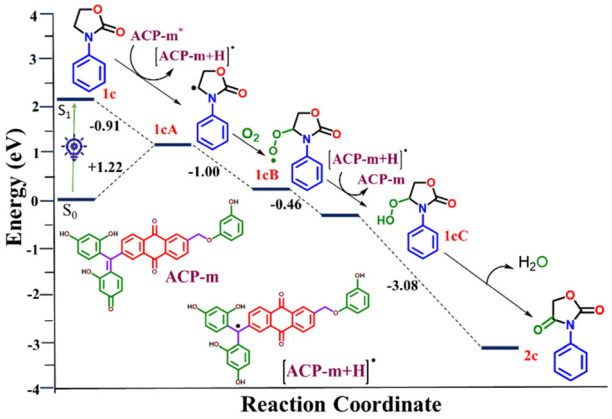

Fig. 5 The proposed mechanism, according to DFT results for oxazolidinone **1c** oxidation by ACP, with potential energy differences of the respective intermediates.

a result, the excited catalyst abstracts a proton more easily, leading to a faster reaction and higher yield. In the reaction mechanism, the rate-determining step is the transfer of the hydrogen atom from oxazolidinone to the catalyst. Thus, the higher acidity of substrates connected with electron-withdrawing aromatic moieties leads to the formation of the desired product with a higher yield.

To better understand the oxidation of 2-oxazolidinone, we have evaluated the course of reaction ACP using DFT calculations at B3LYP/6-311G(d,p)//B3LYP/6-31G(d). ACP was modelled using the representative unit of polymer (ACP-m) as shown in Fig. 4, and 3-phenyloxazolidin-2-one (**1c**) was taken as a model substrate (Fig. 5). The catalyst ACP-m forms [ACP-m + H]$^{\bullet}$ after PCET from substrate **1c**, and the corresponding radical **1cA** is generated, which is lower in energy by 0.91 eV compared to the first singlet excited state of ACP-m. The lowest energy position of **1cA** (ΔE = +1.22 eV) corresponds to the structure in which the hydrogen atom is attached to the quinone unit (represented by [ACP-m + H]$^{\bullet}$). Intermediate **1cA** reacts quickly with O_2 to form the second intermediate **1cB** (ΔE = −1.0 eV). **1cB** recovers a H-atom from [ACP-m + H]$^{\bullet}$ and generates a hydroperoxide intermediate **1cC** (ΔE = −0.46 eV), from which a water molecule is eliminated, and **2c** is produced (ΔE = −3.08 eV). The overall process is downhill with respect to the excited state catalyst and substrate.

In summary, the anthraquinone-resorcinol-based donor–acceptor photocatalyst (ACP), which is readily synthesized through a condensation reaction, efficiently promotes the oxidation of oxazolidinone and its derivatives under blue light irradiation. Upon excitation with visible light, the catalyst can generate singlet oxygen ($^1O_2$) *via* the energy transfer process, contributing to substrate oxidation. However, the major pathway responsible for this oxidation is proton-coupled electron transfer (PCET) from the substrate to the catalyst. The donor–acceptor (D–A) polymer framework enhances photocatalytic performance by functioning as a photobase. The D–A configuration of the polymer facilitates the generation of a charge-separated state that promotes the PCET process by stabilizing the hole (h^+) on the donor unit and the electron (e^-) on the acceptor unit. This work offers valuable insight into achieving demanding transformations through PCET using a heterogeneous D–A polymer-based photocatalyst.

This work has been financially supported by SERB (ANRF), India, vide CRG/2023/004884.

Conflicts of interest

There are no conflicts to declare.

Data availability

The data supporting this article have been included as part of the SI: experimental procedures, analytical data, and NMR spectra. See DOI: https://doi.org/10.1039/d5cc03245h.

Notes and references

1 W. Löscher and P. Klein, *CNS Drugs*, 2021, **35**, 1033–1034.
2 P. C. Unangst, *et al.*, *J. Med. Chem.*, 1994, **37**, 322–328.
3 D. A. Heerding, *et al.*, *Bioorg. Med. Chem. Lett.*, 2003, **13**, 3771–3773.
4 J. A. Sternberg, *et al.*, *Pest Manage. Sci.*, 2001, **57**, 143–152.
5 C. Yang, *et al.*, *Bioorg. Med. Chem. Lett.*, 2013, **23**, 4388–4392.
6 J.-C. Gramain and R. Remuson, *J. Chem. Soc. Perkin Trans. 1*, 1982, 2341.
7 Y. Cao, *et al.*, *Tetrahedron*, 2005, **61**, 6854–6859.
8 A. Galushchinskiy, *et al.*, *Angew. Chem., Int. Ed.*, 2023, **62**, e202301815.
9 X. Fan, *et al.*, *Angew. Chem., Int. Ed.*, 2018, **57**, 8514–8518.
10 Z. Wang, *et al.*, *ACS Appl. Mater. Interfaces*, 2021, **13**, 25898–25905.
11 M.-J. Zhou, *et al.*, *J. Am. Chem. Soc.*, 2021, **143**, 16470–16485.
12 Z. Xu, *et al.*, *Mol. Catal.*, 2021, **514**, 111785.
13 S. P. Pitre, *et al.*, *ACS Omega*, 2016, **1**, 66–76.
14 C. K. Prier, *et al.*, *Chem. Rev.*, 2013, **113**, 5322–5363.
15 C.-X. Chen, *et al.*, *Environ. Sci. Ecotechnol.*, 2024, **22**, 100449.
16 Z. Wang, *et al.*, *Chem. Sci.*, 2024, **15**, 4920–4925.
17 J. I. Bardagi, *et al.*, *Eur. J. Org. Chem.*, 2018, 34–40.
18 I. Itoh, *et al.*, *Tetrahedron Lett.*, 2014, **55**, 3160–3162.
19 L. Capaldo, *et al.*, *Chem. Rev.*, 2022, **122**, 1875–1924.
20 J. Cervantes-González, *et al.*, *ChemCatChem*, 2020, **12**, 3811–3827.
21 C. Wang, X. Zhang and Y. Liu, *Appl. Surf. Sci.*, 2015, **358**, 28–45.
22 I. Ghosh, *et al.*, *Science*, 2014, **346**, 725–728.
23 D. Petzold and B. König, *Adv. Synth. Catal.*, 2018, **360**, 626–630.
24 A. V. Munde, *et al.*, *J. Mater. Chem. A*, 2024, **12**, 18433–18439.
25 W. Huang, *et al.*, *Synthesis*, 2008, 1342–1344.
26 S. Biswas, *et al.*, *Sci. Rep.*, 2018, **8**, 13649.
27 K. C. Nicolaou and C. J. N. Mathison, *Angew. Chem., Int. Ed.*, 2005, **44**, 5992–5997.
28 C. Mei, Y. Hu and W. Lu, *Synthesis*, 2018, 2999–3005.
29 S. Das, *et al.*, *ACS Catal.*, 2021, **11**, 1593–1603.
30 G. Bettoni, *et al.*, *Tetrahedron*, 1981, **37**, 4159–4164.
31 D. Jiang, *et al.*, *Renewable Energy*, 2021, **174**, 928–938.